A Study of Injection Pulling and Locking in Oscillators

Behzad Razavi
Electrical Engineering Department
University of California, Los Angeles

Abstract

This paper presents an analysis that confers new insights into injection pulling and locking of oscillators and the reduction of phase noise under locked condition. A graphical interpretation of Adler's equation predicts the behavior of injection-pulled oscillators in time and frequency domains. An identity derived from the phase and envelope equations expresses the required oscillator nonlinearity across the lock range.

I. Introduction

The phenomenon of injection locking was observed as early as the 17th century, when Christian Huygens, confined to bed by illness, noticed that the pendulums of two clocks on the wall moved in unison if the clocks were hung close to each other [1]. Attributing the coupling to mechanical vibrations transmitted through the wall, Huygens was able to explain the locking between the two clocks.[1]

Injection pulling and locking can occur in any oscillatory system, including lasers, electrical oscillators, and mechanical and biological machines. For example, humans left in isolated bunkers reveal a free-running sleep-wake period of about 25 hours [2], but, when brought back to nature, they are injection-locked to the Earth's cycle.

This paper deals with the study of injection pulling and locking in oscillators, presenting new insights that prove useful in circuit and system design. Section II describes examples wherein injection pulling becomes critical. Following qualitative observations in Section III, Section IV provides a detailed analysis leading to Adler's equation [3] and employs a new graphical interpretation to predict the time- and frequency-domain behavior of pulled oscillators. Sections V and VI deal with the effect of oscillator nonlinearity and phase noise, respectively.

II. Motivation

Analog and mixed-signal systems containing oscillators must often deal with the problem of injection pulling. A few examples demonstrate the difficulty.

Consider the broadband transceiver shown in Fig. 1. Here, a phase-locked loop including VCO_1 provides a retiming clock

[1]Huygens is known for inventing the pendulum clock, discovering the nature of the rings around Saturn, and numerous other accomplishments.

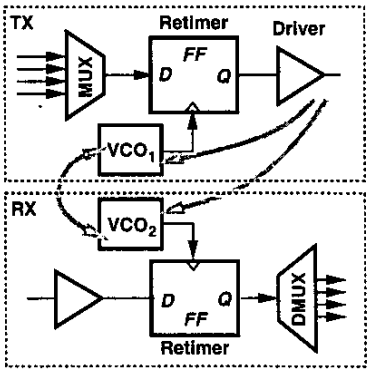

Fig. 1. Injection pulling in a broadband transceiver.

for the transmitted data, which is subsequently amplified by the driver to deliver large currents or voltages to a low-impedance load, e.g., a laser or a 50-Ω line. The receive path incorporates VCO_2 in a clock and data recovery loop. In practice, VCO_1 is phase-locked to a local crystal oscillator, and VCO_2 to incoming data. As a result, the two oscillators may operate at slightly different frequencies, suffering from injection pulling due to substrate coupling. Similarly, the high-swing broadband data at the output of the TX driver may contain substantial energy in the vicinity of the oscillation frequencies of VCO_1 and VCO_2, thus pulling both.

Another example of pulling arises in RF transceivers if the power amplifier (PA) output spectrum lies close to the frequency of an oscillator (Fig. 2). The large swings produced

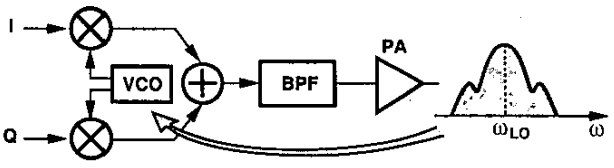

Fig. 2. Injection pulling in an RF transceiver.

by the PA couple to the oscillator through the substrate or the package, leading to considerable pulling.

While injection pulling typically proves undesirable, injection *locking* can be exploited as a useful design technique. For example, an oscillator running at ω_0 can be locked to a signal at $2\omega_0$ to perform frequency division [4, 5, 6]. Similarly, two identical oscillators operating at ω_0 can be locked

0-7803-7842-3/03/$17.00 © 2003 IEEE IEEE 2003 CUSTOM INTEGRATED CIRCUITS CONFERENCE

to the differential phases of a signal at $2\omega_0$, thereby providing quadrature phases [7]. Injection locking must nonetheless deal with the problem of frequency mismatches or errors resulting from inaccurate device models and process and temperature variations.

III. Qualitative Analysis

How does an oscillator operating at ω_0 respond if a periodic waveform at a frequency near ω_0 is injected into it? We answer this question with the aid of some observations.

Consider the simple, conceptual oscillator shown in Fig. 3(a), where other parasitics are neglected, the tank operates

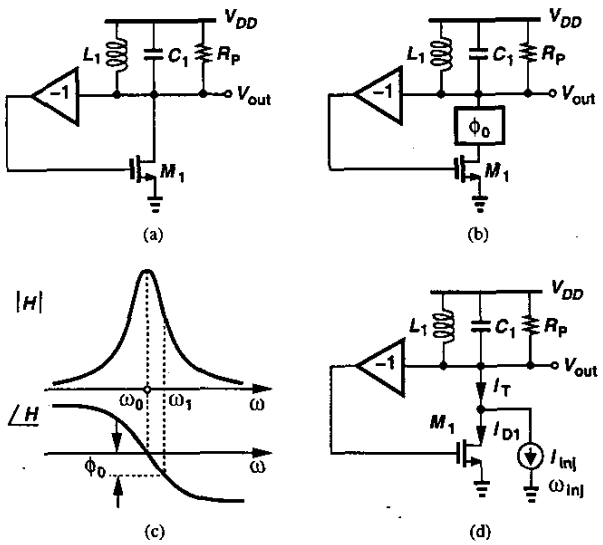

Fig. 3. (a) Simple LC oscillator, (b) frequency shift due to additional phase shift, (c) open-loop characteristics, (d) frequency shift by injection.

at the resonance frequency $\omega_0 = 1/\sqrt{L_1C_1}$, and the inverting buffer follows the tank to create a total phase shift of 360° around the feedback loop. What happens if an additional phase shift is inserted in the loop, e.g., as depicted in Fig. 3(b)?[2] The circuit can no longer oscillate at ω_0 because the total phase shift at this frequency deviates from 360° by ϕ_0. Thus, the oscillation frequency must change such that the tank contributes enough phase shift to cancel the effect of ϕ_0 [Fig. 3(c)]. Since for a second-order tank, $Q = (\omega_0/2)(d\phi/d\omega)$, where $\phi = \angle H(j\omega)$, we obtain the frequency deviation as:

$$\omega_1 - \omega_0 \approx \frac{\phi_0\omega_0}{2Q}. \tag{1}$$

Now suppose we attempt to produce ϕ_0 by *adding* a sinusoidal current to the drain current of M_1 [Fig. 3(d)]. If the amplitude and frequency of I_{inj} are chosen properly, the circuit indeed oscillates at ω_{inj}, with the resultant of I_{D1} and I_{inj} exhibiting a phase that cancels the phase shift introduced by the tank. We say the oscillator is injection-locked to I_{inj}.

[2]Such a phase shift can be produced by adding a cascode device in the current path.

It is interesting to note that, if $\omega_{inj} \neq \omega_0$ (i.e., the tank needs to contribute phase shift), then V_{out} and I_{inj} *must* sustain a finite phase difference. As shown in Fig. 4(a), this is because I_{D1} and V_{out} are aligned, requiring a phase difference between

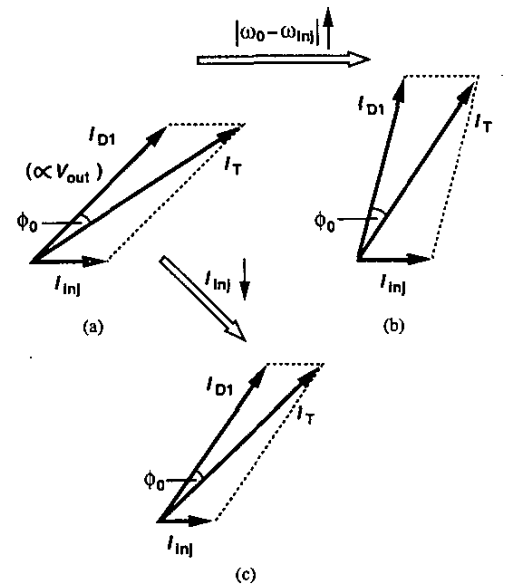

Fig. 4. Phase relationship between input and output for different values of $|\omega_0 - \omega_{inj}|$ and I_{inj}.

I_{D1} and I_{inj} so that I_T can generate V_{out} after rotating through the tank.

How far can ω_{inj} deviate from ω_0 while maintaining lock? To absorb the increasingly greater phase shift produced by the tank, the I_{D1} phasor in Fig. 4(a) must form a larger angle with respect to I_{inj} [Fig. 4(b)]. This trend continues until I_{D1} is perpendicular to I_{inj} and ϕ_0 reaches a maximum. (If I_{D1} further rotates counterclockwise, ϕ_0 begins to decrease.) We then surmise that the circuit begins to lose lock if the phase difference between I_{inj} and V_{out} approaches 90°. This can also be seen in the time domain: if the zero crossings of I_{inj} coincide with the peaks of I_{D1}, no phase synchronization can occur.

How does the amplitude of I_{inj} affect the lock range? We note from Fig. 4(c) that, as I_{inj} decreases, I_{D1} forms a greater angle, thus bringing the lock closer to failure. The lock range is therefore expected to be proportional to the injection level.

As our next step, we move ω_{inj} from *outside* the lock range towards it. The injected signal experiences regeneration around the oscillator loop and can thus be amplified. For an open-loop transfer function $H(s)$, $I_{inj} = I_{inj,p}\cos\omega_{inj}t$ is shaped by

$$\left|\frac{V_{out}}{I_{inj}}(j\omega_{inj})\right| \approx \frac{1}{\left|(\omega_{inj}-\omega_0)\dfrac{dH}{d\omega}\right|}, \tag{2}$$

where ω_{inj} is assumed to be close to ω_0 [8]. If the oscillator of

Fig. 3(d) operates with a unity loop gain, $g_{m1}R_P = 1$,[3] then:

$$\left|\frac{V_{out}}{I_{inj}}(j\omega_{inj})\right| \approx \frac{\omega_0}{2Q|\omega_{inj}-\omega_0|}R_P. \quad (3)$$

In other words, as ω_{inj} approaches ω_0, the injected signal circulates around the loop with a larger amplitude, "hogging" a greater fraction of the available power. We then expect that the component at ω_0 begins to lose energy to that at ω_{inj}, eventually *vanishing* if the latter is sufficiently close. This corresponds to injection locking.

Let us now compute the injection level and frequency such that the amplified input reaches an amplitude equal to that of the free-running oscillator. For the circuit of Fig. 3(d), the oscillation amplitude is approximately equal to $I_{osc,p}R_P$, where $I_{osc,p}$ denotes the peak excursion in the transistor drain current. Equating V_{out} from (3) to $I_{osc,p}R_P$, we obtain,

$$|\omega_{inj}-\omega_0| = \frac{1}{2Q}\frac{I_{inj,p}}{I_{osc,p}}\omega_0. \quad (4)$$

As we will see later, once ω_{inj} enters the range given by this equation, the circuit locks to the input. In other words, injection-locking occurs if the oscillator amplifies the input so much as to raise its level to that of the free-running circuit.

IV. First-Order Analysis

With the foregoing observations in mind, we can now consider a more general LC oscillator under injection.

A. Assumptions

In order to arrive at a mathematically-tractable formulation, we make the following assumptions: (1) the injection level is much less than the free-running oscillation amplitude; (2) the input frequency is close to ω_0, i.e., $|\omega_{inj}-\omega_0| \ll \omega_0/Q$; (3) the input is an unmodulated sinusoid.

For subsequent derivations, we need an expression for the phase shift introduced by a tank in the vicinity of resonance. The circuit of Fig. 5 exhibits a phase shift of

$$\theta = \frac{\pi}{2} - \tan^{-1}\left(\frac{L\omega}{R_P}\cdot\frac{\omega_0^2}{\omega_0^2-\omega^2}\right). \quad (5)$$

Since $\omega_0^2-\omega^2 \approx 2\omega_0(\omega_0-\omega)$, $L\omega/R_P = 1/Q$, and $\pi/2 - \tan^{-1}x = \tan^{-1}(x^{-1})$, we have

$$\tan\theta \approx \frac{2Q}{\omega_0}(\omega_0-\omega). \quad (6)$$

If the input current in Fig. 5 contains phase modulation, i.e., $I_{in} = I_0\cos[\omega t+\psi(t)]$, then the phase shift can be obtained by replacing ω in Eq. (6) with the instantaneous input frequency, $\omega + d\psi/dt$:

$$\tan\theta \approx \frac{2Q}{\omega_0}(\omega_0-\omega-\frac{d\psi}{dt}). \quad (7)$$

Valid for narrowband phase modulation (slowly-varying ψ), this approximation holds well for typical injection phenomena.

[3]Even for large-signal oscillation, we can assume the "average" value of g_m is equal to R_P^{-1}.

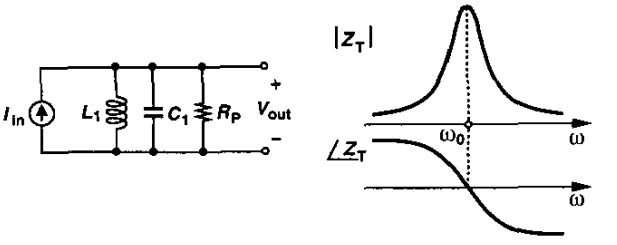

Fig. 5. Phase shift in a tank around resonance.

B. Oscillator under Injection

The objective of our analysis is to determine the effect of injection on the phase and envelope of the oscillator output. In this section, we deal with the phase response - the more important aspect.

Consider the feedback oscillatory system shown in Fig. 6, where the injection is modeled as an additive input. The

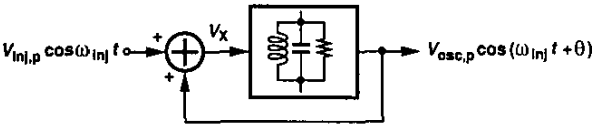

Fig. 6. Oscillatory system under injection.

output is represented by a phase-modulated signal having a carrier frequency of ω_{inj} (rather than ω_0). In other words, the output is assumed to track the input except for a (possibly time-varying) phase difference. This representation is justified later.

The output of the adder is equal to:

$$\begin{aligned} V_X &= V_{inj,p}\cos\omega_{inj}t + V_{osc,p}\cos(\omega_{inj}t+\theta) \quad (8)\\ &= (V_{inj,p}+V_{osc,p}\cos\theta)\cos\omega_{inj}t \\ &- V_{osc,p}\sin\theta\sin\omega_{inj}t. \quad (9)\end{aligned}$$

Factoring $V_{inj,p}+V_{osc,p}\cos\theta$ and defining

$$\tan\psi = \frac{V_{osc,p}\sin\theta}{V_{inj,p}+V_{osc,p}\cos\theta}, \quad (10)$$

we write

$$V_X = \frac{V_{inj,p}+V_{osc,p}\cos\theta}{\cos\psi}\cos(\omega_{inj}t+\psi). \quad (11)$$

Since $\cos\psi = (\sqrt{1+\tan^2\psi})^{-1}$ and $V_{inj,p} \ll V_{osc,p}$, we have $\cos\psi \approx (V_{inj,p}+V_{osc,p}\cos\theta)/\sqrt{V_{osc,p}^2+2V_{osc,p}V_{inj,p}\cos\theta}$, and hence

$$\begin{aligned} V_X &\approx \sqrt{V_{osc,p}^2+2V_{osc,p}V_{inj,p}\cos\theta}\cos(\omega_{inj}t+\psi) \\ &\approx V_{osc,p}\cos(\omega_{inj}t+\psi). \quad (12)\end{aligned}$$

Upon traveling through the LC tank, this signal experiences a phase shift given by (7):

$$V_{out} \approx V_{osc,p}\cos\{\omega_{inj}t + \psi + \tan^{-1}\left[\frac{2Q}{\omega_0}(\omega_0 - \omega_{inj} - \frac{d\psi}{dt})\right]\}. \quad (13)$$

Equating this result to $V_{osc,p}\cos(\omega_{in}t + \theta)$, we obtain

$$\psi + \tan^{-1}\left[\frac{2Q}{\omega_0}(\omega_0 - \omega_{inj} - \frac{d\psi}{dt})\right] = \theta. \quad (14)$$

We also note from (10) that

$$\frac{d\psi}{dt} = \frac{V_{osc,p}^2 + V_{osc,p}V_{inj,p}\cos\theta}{V_{osc,p}^2 + 2V_{osc,p}V_{inj,p}\cos\theta + V_{inj,p}^2}\frac{d\theta}{dt} \approx \frac{d\theta}{dt}, \quad (15)$$

and

$$\tan(\theta - \psi) = \frac{V_{inj,p}\sin\theta}{V_{osc,p} + V_{inj,p}\cos\theta} \quad (16)$$

$$\approx \frac{V_{inj,p}}{V_{osc,p}}\sin\theta. \quad (17)$$

It follows from (14), (15), and (17) that

$$\frac{d\theta}{dt} = \omega_0 - \omega_{inj} - \frac{\omega_0}{2Q}\cdot\frac{V_{inj,p}}{V_{osc,p}}\sin\theta. \quad (18)$$

Originally derived by Adler [3] using a somewhat different approach, this equation serves as a versatile and powerful expression for the behavior of oscillators under injection.

C. Injection Locking

For the oscillator to lock to the input, the phase difference, θ, must remain constant with time. Adler's equation therefore requires that:

$$\omega_0 - \omega_{inj} - \frac{\omega_0}{2Q}\cdot\frac{V_{inj,p}}{V_{osc,p}}\sin\theta = 0. \quad (19)$$

Since $|\sin\theta| \leq 1$, the condition for lock emerges as:

$$|\omega_0 - \omega_{inj}| \leq \frac{\omega_0}{2Q}\cdot\frac{V_{inj,p}}{V_{osc,p}}, \quad (20)$$

which is the same as that expressed by Eq. (4). We denote $[\omega_0/(2Q)](V_{inj,p}/V_{osc,p})$ by ω_L with the understanding that the overall lock range is in fact $\pm\omega_L$ around ω_0.[4]

This study confirms the hypothesis illustrated in Fig. 3: injection locking is simply a shift in the oscillation frequency in response to the additional phase shift that arises from adding an external signal to the feedback signal.

Several important conclusions can be drawn from these equations. First, low-Q oscillators such as resistively-loaded ring topologies are more prone to injection locking (and pulling), underscoring the importance of LC oscillators.

Second, suppose an LC oscillator having a free-running frequency of ω_0 is redesigned to operate at $2\omega_0$ by halving both the tank inductance and the tank capacitance. In the ideal case, the Q of the inductor is doubled at $2\omega_0$, resulting in *the same* lock range as that for oscillation at ω_0 if $V_{inj,p}/V_{osc,p}$ remains constant. This is an alarming result as it predicts that the *relative* injection lock range, $|\omega_0 - \omega_{inj}|/\omega_0$, becomes narrower at high frequencies. For example, quadrature oscillators may face more severe trade-offs due to this trend.

Third, injection locking to a frequency $\omega_{inj} \neq \omega_0$ mandates operation away from the tank resonance, where the Q begins to degrade. This is in stark contrast to phase-locking, in which case the oscillation frequency can be varied (e.g., by a varactor) while maintaining the tank at resonance.

Fourth, Eq. (19) confirms the trend predicted by Fig. 4, indicating that injection locking is accompanied by a static phase error:

$$\theta = \sin^{-1}\frac{\omega_0 - \omega_{inj}}{\omega_L}, \quad (21)$$

which, as depicted in Fig. 7, reaches $\pm\pi/2$ at the edges of the lock range. As mentioned in Section II, at $\theta = \pm\pi/2$, the zero crossings of the input fail to synchronize the oscillator.

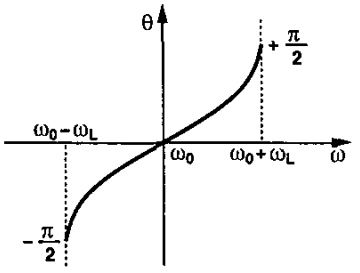

Fig. 7. Phase shift in an injection-locked oscillator.

Varying with process and temperature to some extent, θ may prove problematic if the phase relationship between the input and the output is critical in an application. For example, if an injection-locked oscillator serves as a frequency divider in a tree multiplexer or demultiplexer environment, then the variation of the phase becomes undesirable.

D. Injection Pulling

If the injected signal frequency falls out of, but not very far from, the lock range, then the oscillator is "pulled." This behavior can be studied by solving Adler's equation with the assumption $|\omega_0 - \omega_{inj}| > \omega_L = [\omega_0/(2Q)](V_{inj,p}/V_{osc,p})$. Note from (18) that $d\theta/dt$ reaches a maximum of $\omega_0 - \omega_{inj} + \omega_L$, a small value compared to ω_0. Similarly, higher derivatives of θ are also small. That is, θ indeed varies slowly.

Adler's equation can be rewritten as:

$$\frac{d\theta}{\omega_0 - \omega_{inj} - \omega_L\sin\theta} = dt. \quad (22)$$

[4] We call ω_L the "one-sided" lock range.

Noting that $\sin\theta = 2\tan(\theta/2)/[1+\tan^2(\theta/2)]$, making a change of variable $\tan(\theta/2) = u$, and carrying out the integration, we arrive at:

$$\tan\frac{\theta}{2} = \frac{\omega_L}{\omega_0 - \omega_{inj}} + \frac{\omega_b}{\omega_0 - \omega_{inj}}\tan\frac{\omega_b t}{2}, \qquad (23)$$

where $\omega_b = \sqrt{(\omega_0 - \omega_{inj})^2 - \omega_L^2}$. This paper introduces a graphical interpretation of this equation that confers a great deal of insight into the phenomenon of injection pulling.

Case I: Quasi-Lock Let us first examine the above result for an input frequency just below the lock range, i.e., $\omega_{inj} < \omega_0 - \omega_L$ but $(\omega_0 - \omega_{inj})/\omega_L \approx 1$. Under this condition, ω_b is relatively small, and the right hand side of Eq. (23) is dominated by the first term (≈ 1) so long as $\tan(\omega_b t/2)$ is less than one, approaching a large magnitude only for a short duration [Fig. 8(a)]. Noting that the cycle repeats with a period equal to ω_b, we plot θ as shown in Fig. 8(b). The key

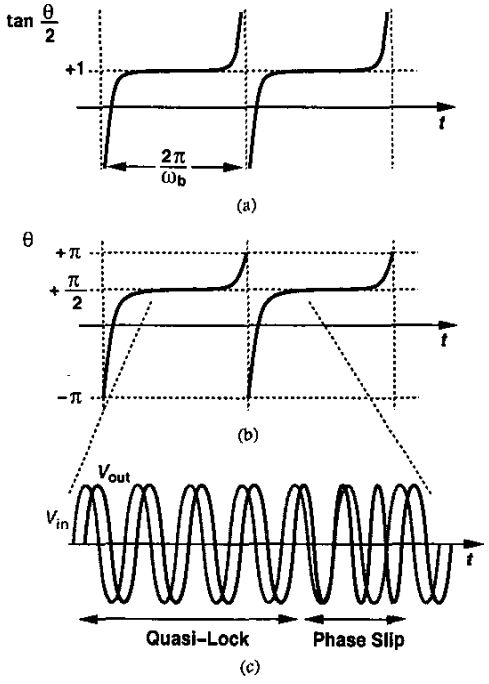

Fig. 8. Phase variation of an injection-pulled oscillator.

observation here is that θ is near 90° most of the time - as if the oscillator were injection-locked to the input at the edge of the lock range. At the end of each period and the beginning of the next period, θ undergoes a rapid 360° change and returns to the quasi-lock condition [Fig. 8(c)].

We now study the spectrum of the pulled oscillator. The spectrum has been analytically derived using different techniques [9, 10], but additional insight can be gained if the results in Fig. 8 are utilized as the starting point. The following observations can be made. (1) The periodic variation of θ at a rate of ω_b implies that the output beats with the input, exhibiting sidebands with a spacing of ω_b. Note that ω_b is a function of both $\omega_0 - \omega_{inj}$ and ω_L (and hence the injection level). (2) Since the oscillator is almost injection-locked to the input for a large fraction of the period, we expect the spectrum to contain significant energy at ω_{inj}. (3) Writing the instantaneous frequency of the output as $d(\omega_{inj}t + \theta)/dt = \omega_{inj} + d\theta/dt$ and redrawing Fig. 8(b) with the modulo-2π transitions at the end of each period removed [Fig. 9(a)], we obtain the

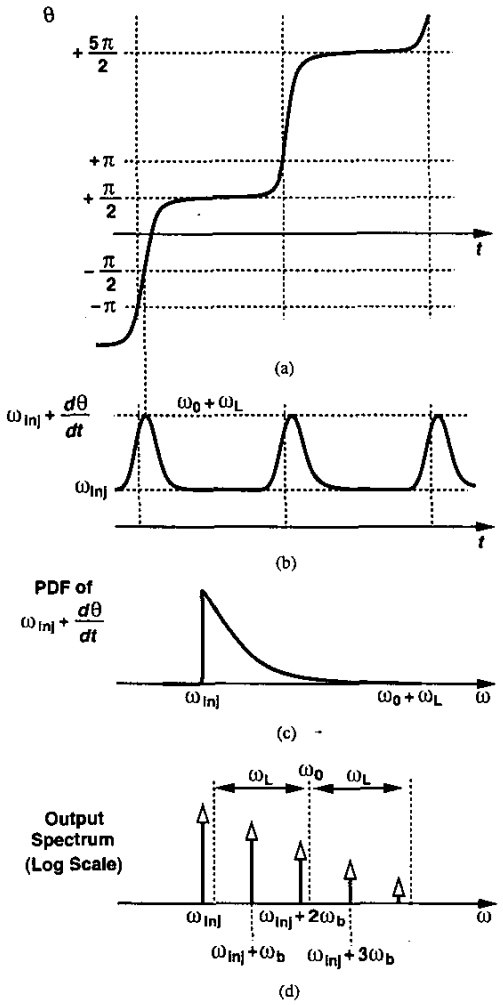

Fig. 9. Instantaneous frequency and spectrum of an injection-pulled oscillator.

result depicted in Fig. 9(b). The interesting point here is that, for ω_{inj} *below* the lock range, the instantaneous frequency of the oscillator goes only *above* ω_{inj}, exhibiting a peak value of $\omega_0 + \omega_L$ as obtained from Eq. (18). That is, the output spectrum contains mostly sidebands above ω_{inj}.

We now invoke a useful observation that the shape of the spectrum is given by the probability density function (PDF) of the instantaneous frequency [11]. The PDF is qualitatively plotted in Fig. 9(c), revealing that most of the energy is confined to the range $[\omega_{inj} \quad \omega_0 + \omega_L]$ and leading to the actual spectrum in Fig. 9(d). The magnitude of the sidebands drops

approximately linearly on a logarithmic scale [9, 10].

Is it possible for one of the sidebands to fall at the natural frequency, ω_0? The following must hold: $\omega_0 = \omega_{inj} + n\omega_b$, where n is an integer. Thus, $(\omega_0 - \omega_{inj})^2/\omega_L^2 = 1 - 1/n^2$. Since ω_{inj} is out of the lock range, the left side of this equation exceeds unity and no value of n can place a sideband at ω_0. We therefore say the oscillator is "pulled" from its natural frequency. This also justifies the use of ω_{inj} - rather than ω_0 - for the carrier frequency of the output.

Case II: Fast Beat It is instructive to examine the results obtained above as ω_{inj} deviates farther from the lock range while other parameters remain constant. Rewriting Eq. (23) as

$$\tan\frac{\theta}{2} = \frac{\omega_L}{\omega_0 - \omega_{inj}} + \sqrt{1 - \frac{\omega_L^2}{(\omega_0 - \omega_{inj})^2}}\tan\frac{\omega_b t}{2}, \quad (24)$$

we recognize that the vertical offset decreases whereas the slope of the second term increases. The right hand side therefore appears as depicted in Fig. 10(a), yielding the behavior shown in Fig. 10(b) for θ. Thus, compared to the case illustrated in Fig. 8, (1) the beat frequency increases, leading to a wider separation of sidebands; (2) θ stays relatively constant for a shorter part of the period and exhibits a faster variation at the beginning and end; (3) the instantaneous frequency is around ω_{inj} for a shorter duration [Fig. 10(c)], producing a smaller spectral line at this frequency. In fact, if ω_{inj} is sufficiently far from ω_0, the energy at ω_{inj} falls below that at the next sideband $(\omega_{inj} + \omega_b)$ [Fig. 10(d)]. Eventually, the components at ω_{inj} and $\omega_{inj} + 2\omega_b$ exhibit approximately equal levels [9, 10].

Interestingly, the analyses in [9, 10] only reveal the spectrum in Fig. 10(d). On the other hand, the approach presented here, particularly the use of the PDF of the instantaneous frequency, correctly predicts both quasi-lock and fast beat conditions. This is evidenced by the measured results shown in Fig. 11 for a 1-GHz CMOS LC oscillator.

In quadrature oscillators, pulling may occur if the frequency mismatch between the two cores exceeds the injection lock range. With insufficient coupling, the oscillators display a behavior similar to that depicted in Figs. 8 and 10. Note that the resulting sidebands are *not* due to intermodulation between the two oscillator signals. For example, the spacing between the sidebands is a function of the coupling factor.

V. Effect of Oscillator Nonlinearity

Our analysis of injection locking and pulling has thus far ignored nonlinearities in the oscillator. While this may imply that a "linear" oscillator[5] can be injection pulled or locked, we know from the superposition principle that this cannot happen. Specifically, superposition of an initial condition (to define the oscillation amplitude) and the injected signal does not lead to

[5]A linear oscillator can be defined as on in which the loop gain is exactly unity for all signal levels.

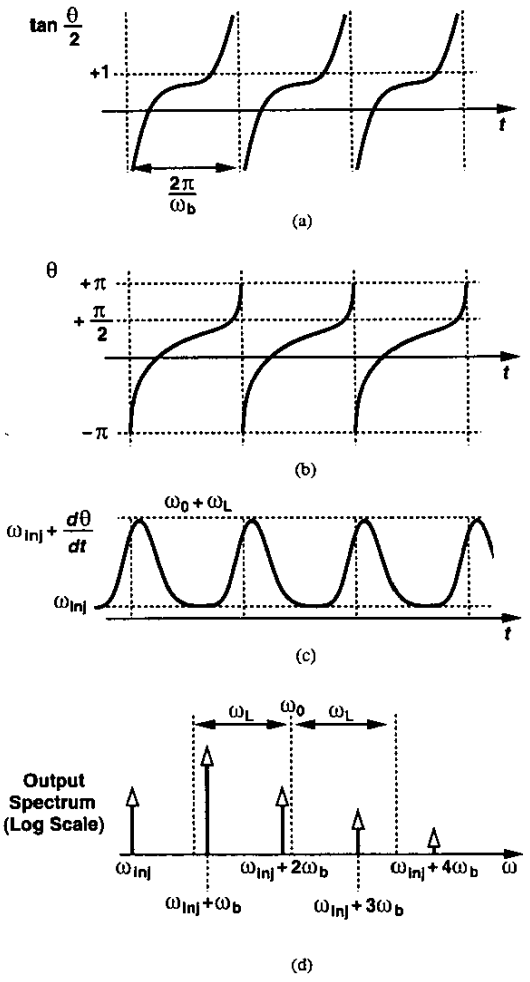

Fig. 10. Pulling behavior for injection somewhat far from the lock range.

pulling or locking. To resolve this paradox, we reexamine the oscillatory system under injection, seeking its envelope behavior.

In this case, it is simpler to model the oscillator as a one-port circuit consisting of a parallel tank and a nonlinear negative conductance, Fig. 12, where $G_1 = R_p^{-1}$. For example, M_1 and the inverting buffer in Fig. 3(a) constitute a negative G_m cell. As we will see, the average value of $-G_m$ varies with I_{inj} and ω_{inj}. For this circuit,

$$C_1\frac{d^2V_{osc}}{dt^2} - (G_1 - G_m)\frac{dV_{osc}}{dt} + \frac{1}{L_1}V_{osc} = \frac{dI_{inj}}{dt}. \quad (25)$$

Now let us assume $I_{inj}(t) = I_{inj,p}\cos\omega_{inj}t = Re\{I_{inj,p}\exp(j\omega_{inj}t)\}$ and $V_{osc}(t) = V_{env}(t)\cos(\omega_{inj}t + \theta) = Re\{V_{env}(t)\exp(j\omega_{inj}t + j\theta)\}$, where $V_{env}(t)$ denotes the envelope of the output. Substituting the exponential terms in

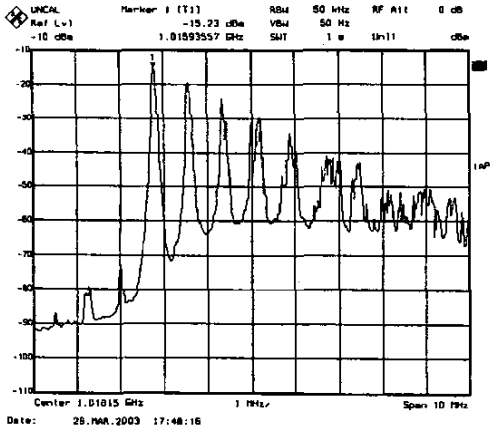

(a)

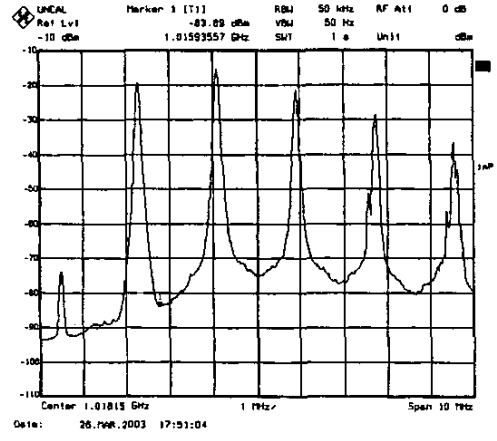

(b)

Fig. 11. Measured pulling behavior for (a) quasi-lock and (b) fast beat conditions.

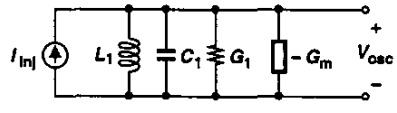

Fig. 12. One-port representation of an oscillator under injection.

(25) and separating the real and imaginary parts, we have,

$$C_1\frac{d^2V_{env}}{dt^2} - C_1(\omega_{inj} + \frac{d\theta}{dt})^2V_{env} + (G_1 - G_m)\frac{dV_{env}}{dt} + \frac{1}{L_1}V_{env} = \omega_{inj}I_{inj,p}\sin\theta \qquad (26)$$

$$2C_1(\omega_{inj} + \frac{d\theta}{dt})\frac{dV_{env}}{dt} + C_1\frac{d^2\theta}{dt^2}V_{env} + (G_1 - G_m)(\omega_{inj} + \frac{d\theta}{dt})V_{env} = \omega_{inj}I_{inj,p}\cos\theta. \qquad (27)$$

To simplify these equations, we assume: (1) the envelope varies slowly and by a small amount; (2) the magnitude of the envelope can be approximated as the tank peak current produced by the $-G_m$ circuit, $I_{osc,p}$, multiplied by the tank resistance, $G^{-1} = QL_1\omega_0$; (3) $\omega_{inj}^2 - \omega_0^2 \approx 2\omega_0(\omega_0 - \omega_{inj})$; (4) $\omega_{inj} \approx \omega_0$ where applicable; (5) the phase and its derivatives vary slowly. Equations (26) and (27) thus reduce to

$$\frac{d\theta}{dt} = \omega_0 - \omega_{inj} - \frac{\omega_0 I_{inj,p}}{2QI_{osc,p}}\sin\theta \qquad (28)$$

$$\frac{dV_{env}}{dt} + \frac{G_1 - G_m}{2C_1}V_{env} = \frac{I_{inj,p}\cos\theta}{2C_1}. \qquad (29)$$

The first is Adler's equation whereas the second expresses the behavior for the envelope.

To develop more insight, let us study these results within the lock range, i.e., if $d\theta/dt = dV_{env}/dt = 0$. Writing $\sin^2\theta + \cos^2\theta = 1$ gives the following useful identity,

$$\left(\frac{\omega_0 - \omega_{inj}}{\omega_L}\right)^2 + \left(\frac{G_1 - G_m}{I_{inj,p}}V_{env,p}\right)^2 = 1. \qquad (30)$$

For $\omega_{inj} = \omega_0$,

$$G_m = G_1 - \frac{I_{inj,p}}{V_{env,p}} \qquad (31)$$

$$= G_1 - \frac{I_{inj,p}}{R_p I_{osc,p}}. \qquad (32)$$

that is, the circuit responds by *weakening* the $-G_m$ circuit (i.e., allowing more saturation) because the injection adds energy to the oscillator. On the other hand, for $|\omega_0 - \omega_{inj}| = \omega_L$, we have $G_m = G_1$, recognizing that the $-G_m$ circuit must be sufficiently strong under this condition. Figure 13 illustrates the behavior of G_m across the lock range.

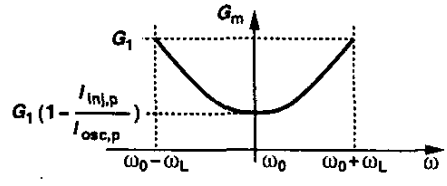

Fig. 13. Behavior of G_m across the lock range.

VI. Phase Noise

The phase noise of oscillators can be substantially reduced by injection locking to a low-noise source. From a time-domain perspective, the "synchronizing" effect of injection manifests itself as correction of the oscillator zero crossings in every period, thereby lowering the accumulation of jitter. This viewpoint also reveals that (1) the reduction of phase noise depends on the injection level, and (2) the reduction reaches a maximum for $\omega_{inj} = \omega_0$ [Fig. 14(a)] (where the zero crossings of I_{inj} greatly impact those of I_{osc}) and a minimum for $\omega_{inj} = \omega_0 \pm \omega_L$ [Fig. 14(b)] (where the zero crossings of I_{inj} coincide with the zero-slope points on I_{osc}).

We present a new analysis of phase noise under injection locking using the the one-port model of Fig. 12 and Eq. (32). As depicted in Fig. 15, the noise of the tank and the

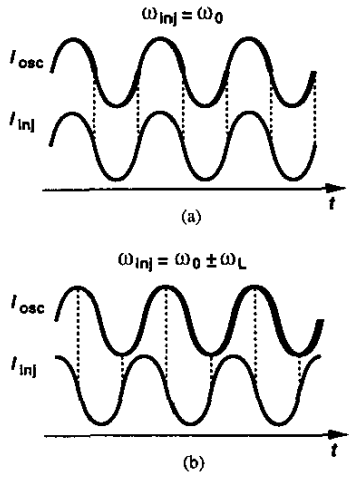

Fig. 14. Effect of injection locking on jitter (a) in the middle and (b) at the edge of the lock range.

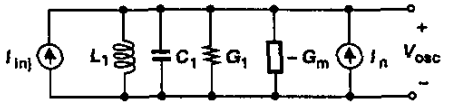

Fig. 15. Model for studying phase noise.

$-G_m$ cell can be represented as a current source I_n. With no injection input, the average value of $-G_m$ cancels G_1, and I_n experiences the noise-shaping function given by Eq. (3). Thus, I_n is amplified by an increasingly higher gain as the noise frequency approaches ω_0.[6]

Now suppose a finite injection with no phase noise is applied at the center of the lock range, $\omega_{inj} = \omega_0$. Then, Eq. (32) predicts that the overall tank admittance rises to $G_1 - G_m = I_{inj,p}/(R_P I_{osc,p})$. In other words, the tank impedance seen by I_n at ω_0 falls from infinity (with no injection) to $R_p I_{osc,p}/I_{inj,p}$ under injection locking. As the frequency of I_n deviates from ω_0, $R_p I_{osc,p}/I_{inj,p}$ continues to dominate the tank impedance up to the frequency offset at which the phase noise approaches that of the free-running oscillator (Fig. 16). To determine this point, we equate the free-running noise shaping function of Eq. (3) to $R_p I_{osc,p}/I_{inj,p}$:

$$\frac{\omega_0}{2Q|\omega_n - \omega_0|} R_p = R_p \frac{I_{osc,p}}{I_{inj,p}}, \tag{33}$$

obtaining

$$|\omega_n - \omega_0| = \frac{\omega_0}{2Q} \cdot \frac{I_{inj,p}}{I_{osc,p}}. \tag{34}$$

Thus, the free-running and locked phase noise profiles meet at the edges of the lock range.

It is interesting to note that the derivations in [12] and [13] conclude that the near-carrier phase noise is nearly equal to that of the synchronizing input and relatively independent of the free-running oscillator phase noise. By contrast, our derivation reveals a significant contribution by the oscillator itself within the lock range and its dependence on the injection level. This has been indeed verified by measurements on a 1-GHz CMOS LC oscillator.

As illustrated in Fig. 14(b), if the input frequency deviates from ω_0, the resulting phase noise reduction becomes less pronounced. This can also be seen from Eq. (30) because $G_1 - G_m$ drops to zero as the input frequency approaches $\omega_0 \pm \omega_L$. General equations for this case and the case of noisy input are given in [12, 13].

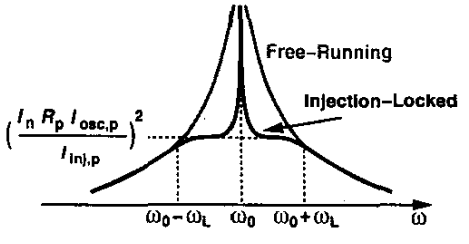

Fig. 16. Reduction of phase noise due to injection locking.

[6]For very small frequency offsets, the noise shaping function assumes a Lorentzian shape and hence a finite value.

REFERENCES

[1] A. E. Siegman, *Lasers*, Mill Valley, CA: University Science Books, 1986.

[2] R. R. Ward, *The Living Clocks*, New York: Alfred Knopf, Inc., 1971.

[3] R. Adler, "A Study of Locking Phenomena in Oscillators ," *Proc. of the IEEE*, vol. 61, No. 10, pp. 1380-1385, Oct. 1973.

[4] V. Manassewitsch, *Frequency Synthesizers*, Third Edition, New York: Wiley, 1987.

[5] E. Normann, "The Inductance-Capacitance Oscillator as a Frequency Divider," *Proc. of IRE*, vol. 24, pp. 799-803, Oct. 1946.

[6] P. G. Sulzer, "Modified Locked-Oscillator Frequency Divider," *Proc. of IRE*, vol. 29, pp. 1535-1537, Dec. 1951.

[7] A. Ravi et al, "An Integrated 10/5GHz Injection-Locked Quadrature LC VCO in a 0.18-um Digital CMOS Process," *Proc. ESSCIRC*, pp. 314-317, September 2002.

[8] B. Razavi, "A Study of Phase Noise in CMOS Oscillators," *IEEE J. Solid-State Circuits*, vol. 31, pp. 331-343, March 1996.

[9] H. L. Stover, "Theoretical Explanation of the Output Spectra of Unlocked Driven Oscillators," *Proc. of IEEE*, vol. 54, pp. 310-311, Feb. 1966.

[10] M. Armand, "On the Output Spectrum of Unlocked Driven Oscillators," *Proc. of IEEE*, vol. 59, pp. 798-799, May 1969.

[11] H. E. Rowe, *Signals and Noise in Communication Systems*, Princeton, NJ: Van Nostrand Company, Inc., 1965.

[12] K. Kurokawa, "Noise in Synchronized Oscillators," *IEEE Tran. MTT*, vol. 16, pp. 234-240, April 1968.

[13] H.-C. Chang et al, "Phase Noise in Externally Injection-Locked Oscillator Arrays," *IEEE Tran. MTT*, vol. 45, pp. 2035-2042, Nov. 1997.